AN ENHANCED SPACE-WISE SIMULATION FOR GOCE DATA REDUCTION

Federica Migliaccio [(1)], Mirko Reguzzoni [(1)], Fernando Sansò [(1)] and Carl Christian Tscherning [(2)]

[(1)] *DIIAR - Sezione Rilevamento - Politecnico di Milano - P.za Leonardo da Vinci, 11 - 20133 Milano - Italy*
[(2)] *Department of Geophysics - University of Copenhagen - Juliane Maries Vej, 30 - 2100 Copenhagen, Denmark*

ABSTRACT

Polar gaps effects, gridding effects and noise propagation from GOCE T_{rr} data into harmonic coefficients estimates, by the so-called space-wise approach, have been extensively studied. To this aim two techniques are possible, namely the fast spherical collocation and the numerical integration. Recently the conclusion has been drawn that the two methods are almost equivalent, though collocation reveals to be more robust against aliasing and polar gaps [9].
Now several generalizations need to be implemented and integrated in order to come to a final architecture of the software. The integration of non-radial components and the effects of small rotations are presented in a parallel paper [10]. In this work we aim at integrating the information coming from T_{rr}, T_r and T data, in order to better understand the improvement in the low frequency band. To obtain this result, we simulated a realistic data grid on a spherical boundary, implementing a realistic (and close to optimal) grid step and including realistic polar gaps effects.

1 THE RATIONALE FOR A JOINT USE OF T_{zz} AND T

Originally this paper was intended to study in numerical terms the joint effects of a number of features of the GOCE mission [4] which are difficult to be analytically studied according to the so-called space-wise approach [8] [11]. Such factors can be: the presence of polar gaps [1] [7], the misalignment of measurement axes with respect to an orbital frame [10] and, specially, the shape of the noise spectrum [3]. At the same time we wanted to improve our simulations by including other functionals of the anomalous potential T, measured during the mission; the first idea was to treat simultaneously T_{zz}, T_z and T. The first quantity comes from the gradiometer, while the second could be derived from a combination of GPS-orbit and accelerometers, like the third which can be achieved by the so-called energy integral approach [5] [14].
Since the parameters of noise statistics have been changed quite recently, due to ESA's decision of dismissing the FEEP (Field Emission Electric Propulsion) system, we decided first of all to test what was the effect of the new error spectrum on the space-wise approach. We simulated a noisy data set of second radial derivatives, i.e. $\underline{Y}_0 = \underline{T}_{rr} + \underline{\nu}$, in order to check the convergence of the space-wise iterative scheme [10]; contrary to the previous behaviour, the iterations show that the "small" perturbative operator has in fact a norm very close to 1 so that convergence is strongly questioned. The reason why this happens can be understood from the iterative formula, which in this case writes

$$\hat{\underline{T}} = S\Phi^c L(\hat{\underline{T}}) + S\Phi\underline{Y}_0 \tag{1}$$

where:

$L(\underline{T}) = T_{rr}$,
Φ = Wiener filter,
Φ^c = complementary Wiener filter = $I - \Phi$,
S = solver = AG,
G = gridder,
A = harmonic analyser.

Note that the iteration in the second member basically tends to reconstitute the low-frequency part of the signal, which is lost by Wiener-filtering.

If one looks then at the new error spectrum as compared to the old one (cf. Fig.1), and one recalls that the Wiener filter is spectrally represented by

$$W(f) = \frac{S(f)}{S(f) + N(f)} \tag{2}$$

where:

$S(f)$ = spectrum of the signal,
$N(f)$ = spectrum of the noise,

one can easily realize that, under the new conditions, $W(f)$ goes close to zero already at $f = 5 \cdot 10^{-4}$ Hz, instead of $f = 10^{-6}$ Hz, shrinking the bandwidth of the filter. In this case therefore the lost part of the signal is too large and the perturbative operator has a much larger norm [2]. So the problem was to increase the information on the low-frequency band of the spectrum; this could be done by joining T_r and T to T_{rr}, into a unique Wiener filter and, since after the first attempts we convinced ourselves that most of the contribution was coming from T, we designed a numerical experiment based on the joint treatment of T_{zz} and T data.

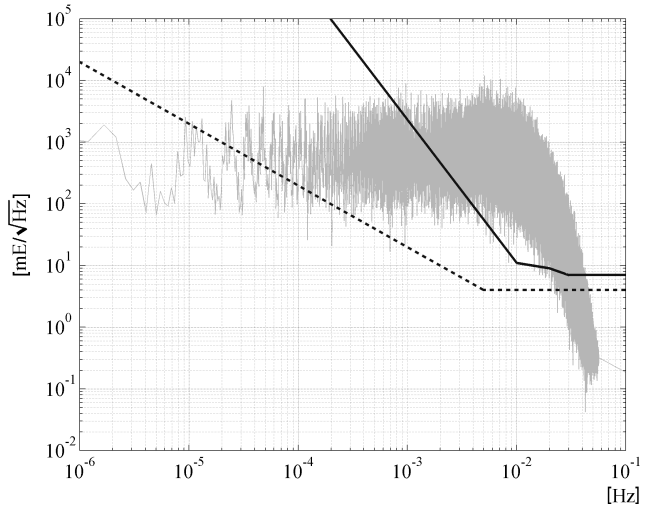

Fig. 1. Signal (in grey) and noise (in black) power spectral density of the T_{zz} component. Original performance (in dashed line) vs. new specification (in solid line).

2 THE SPACE-WISE APPROACH WITH T_{zz} AND T

In abstract form, the space-wise approach with two flows of data has exactly the same justification as with one flow only, the difference being that each step has to be duly justified and written in an extended form.
Just to recall shortly [10] we combine the three equations

$$\begin{cases} \underline{Y}_0 = M(\underline{T}) + \nu & \text{(observation equation)} \\ L(\underline{T}) = D\,M(\underline{T}) + R(\underline{T}) & \text{(rotation equation)} \\ S\,L(\underline{T}) = I & \text{(solver equation)} \end{cases} \tag{3}$$

with the double Wiener filter Φ to get

$$\underline{T} = S\,\Phi^c\,L(\underline{T}) + S\,\Phi\,R(\underline{T}) + S\,\Phi\,D\,\underline{Y}_0 - S\,\underline{e} \tag{4}$$

which is then approximated by putting $\underline{e}$=0 and solved iteratively to estimate the harmonic coefficients $\hat{\underline{T}}$. We have now to specify the meaning of the various symbols in Eq. (3) and Eq. (4); we have

$$M(\underline{T}) = \begin{vmatrix} \vdots \\ T_{zz}(t) \\ T(t) \\ \vdots \end{vmatrix} \qquad L(\underline{T}) = \begin{vmatrix} \vdots \\ T_{rr}(t) \\ T(t) \\ \vdots \end{vmatrix} \qquad (t = 1, 2, \ldots N)$$

$$D = \begin{vmatrix} \ddots & & & 0 \\ & \cos^2\alpha_t \cos^2\beta_t & 0 & \\ & 0 & 1 & \\ 0 & & & \ddots \end{vmatrix} \qquad (\alpha_t, \beta_t \text{ rotations around } x \text{ and } y)$$

$$\Phi = F^{-1} \begin{vmatrix} S_{TrrTrr}(f) & S_{TrrT}(f) \\ S_{TrrT}(f) & S_{TT}(f) \end{vmatrix} \cdot \begin{vmatrix} S_{TrrTrr}(f) + N_{TrrTrr}(f) & S_{TrrT}(f) \\ S_{TrrT}(f) & S_{TT}(f) + N_{TT}(f) \end{vmatrix}^{-1} F$$

$$S = A\ G$$

where:

F = Fourier transform operator,
S_{TrrTrr} , S_{TT} = spectra of T_{rr} and T,
S_{TrrT} = cross-spectrum of T_{rr} and T,
N_{TrrTrr} , N_{TT} = noise spectra of T_{rr} and T.

The core of the space-wise approach is the solver operator S which consists of two stages: the gridder G, reducing the along-orbit data onto a spherical grid, and the harmonic analyser A, recovering the potential coefficients from the gridded data with the use of the fast spherical collocation technique [12] or by integration [6].
Of particular importance has proven to be the choice of the gridder G. We have decided to grid separately T_{rr} and T, both estimated along the orbit by the Wiener filter; this is done by local collocation, cell by cell, on a moving window of double size with respect to the grid cell (cf. Fig.2).
Note that, in the case of harmonic analysis by integration, the grid of T_{rr} and the grid of T give rise to different estimates of the coefficients $\underline{T}$ which are then merged by using as weights the inverse of the variances of the estimation error. On the contrary, this is done in a single step by fast spherical collocation.
Finally the reconstruction operator $R(\underline{T})$ allows to synthesize the potential $T(t)$ and the tensor of its second derivatives along the orbit, which, duly rotated and introduced in the second equation of (3), produces T_{rr} from T_{zz}. In the next paragraph we describe a numerical example applied to equation (4).

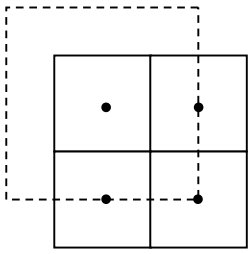

Fig.2. Interpolation scheme: in solid line the final grid and in dashed line the moving window used for estimating the centre value of each cell.

3 THE NUMERICAL SIMULATION

We have simulated observations for a mission length of 100 days, at an altitude of 250 km, by using the EGM96 model up to degree 300. The observations were T_{zz}, along a z-axis oscillating according to the following laws:

$$\theta_\eta = A_\eta \sin \omega_\eta t \qquad A_\eta = 3° \qquad \frac{2\pi}{\omega_\eta} \cong 2\,\text{hours} \qquad (\theta_\eta \text{ rotation around cross - track axis})$$

$$\theta_r = A_r \sin \omega_r t \qquad A_r = 1° \qquad \frac{2\pi}{\omega_r} \cong 1\,\text{hour} \qquad (\theta_r \text{ rotation around radial axis})$$

and T, for every second along the orbit, which was circular, with inclination I=96.5°.
To T_{zz} a coloured noise has been added, specified by the new spectrum in Fig.1, while to T a white noise has been added with power density corresponding to σ=0.3 m^2/s^2 (i.e. to an orbital error of about 3 cm), as shown in Fig.3. The spectra of T_{rr}, T and cross-spectrum of T_{rr} and T have been computed from the model EGM96.
It is interesting to observe that the joint use of T_{rr} and T in the Wiener filter causes the variance of the estimation error of T_{rr} along the orbit to drop from ≅41 mE down to ≅15 mE (cf. Fig.4 and Fig.5); this proves the effectiveness of T in integrating the low frequency information on the spectrum of T_{rr}.
The grids produced were of size 0.72°×0.72° and the local collocation for the computation of T_{rr}, T at each knot used a window of 1.44°×1.44° with data decimated by a factor 4 along each track in the window. The final error of T_{rr} on the spherical grid is about 4.7 mE.
The two different models estimated from T_{rr} and T, using the integration approach, are displayed in Fig.6, showing the well known fact that the satellite-to-satellite tracking data bring more information at low-medium degrees, while the gradiometric data are especially sensitive to the high degrees.
It is also interesting to compare the results of the analysis when we apply the Fast Spherical Collocation method, as opposed to numerical integration; as Fig.7 shows, the two results are similar but not completely equivalent, leaving some room for optimisation.

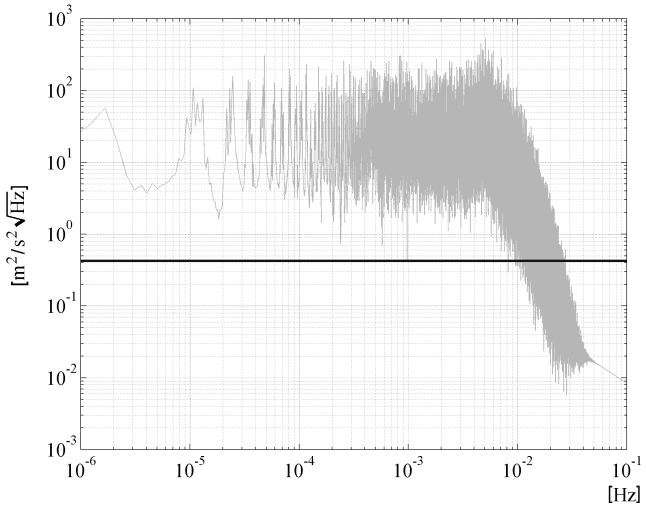

Fig. 3. Signal (in grey) and noise (in black) power spectral density of the potential T.

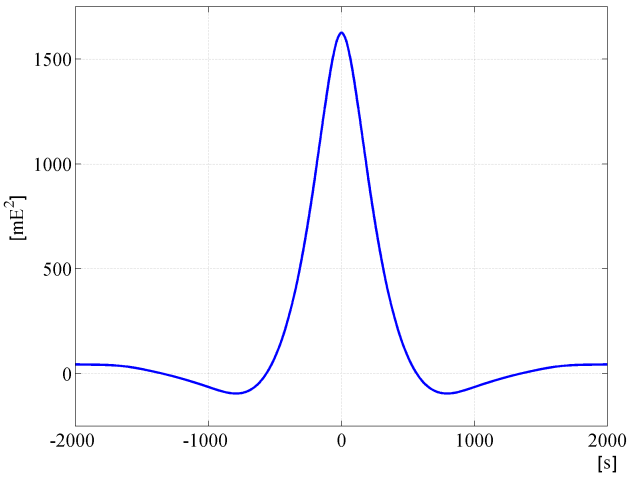

Fig. 4. Covariance function of the T_{rr} estimation error, using a single-input single-output Wiener filter.

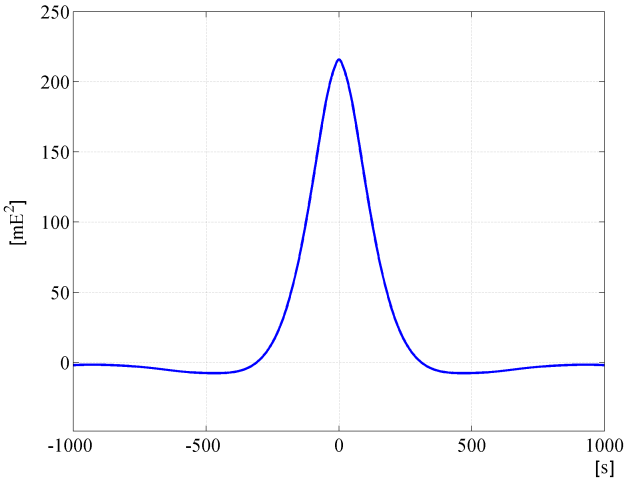

Fig. 5. Covariance function of the T_{rr} estimation error, using a joint Wiener filter between T_{rr} and T.

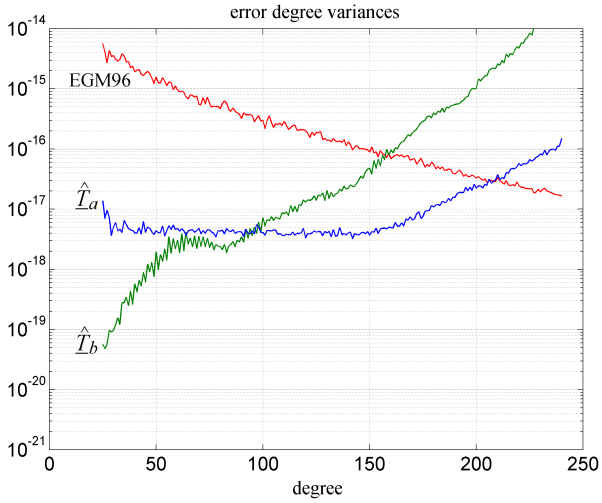

Fig. 6. Estimation error of the harmonic coefficients using numerical integration with T_{rr} gridded data ($\hat{\underline{T}}_a$) and with T gridded data ($\hat{\underline{T}}_b$). The reference model is EGM96.

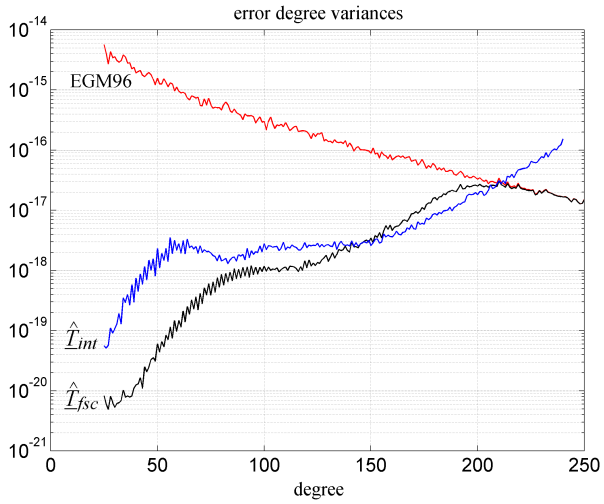

Fig. 7. Final estimation error of the harmonic coefficients using fast spherical collocation ($\hat{\underline{T}}_{fsc}$) and numerical integration ($\hat{\underline{T}}_{int}$). The reference model is EGM96.

4 CONCLUSIONS

The numerical experiment shows that a reasonable reconstruction of the vector of harmonic coefficients can be performed up to degree 210, and since only a 100 days mission has been used we have some hope that a better result can be achieved in the end.

Two remarks are also of some interest here. The first is that by adding T_{xx} to the filtering procedure we do not gain very much, because the Wiener filter has almost the same performance as using T_{zz} and T only. A more relevant improvement is expected by the joint gridding of all the diagonal components of the gravity tensor [13], where the significance of spatial correlation is stronger.

The second remark is that if we tried to use a simple polynomial interpolation as a gridder we would end up with a significantly poorer result, reconstructing the harmonic coefficients only up to degree 190. This shows once more how delicate and important is the phase of spatially mixing the data to obtain the best estimate of the gravity field from GOCE observations.

References

1. Albertella A., Migliaccio F. and Sansò F., *Data gaps in finite dimensional boundary value problems for satellite gradiometry*, Journal of Geodesy, vol. 75, 641-646, 2001.

2. Albertella A., Migliaccio F., Reguzzoni M. and Sansò F., *Spacewise approach and measurement bandwidth in satellite gradiometry*, Bollettino di Geodesia e Scienze Affini, N. 3, 179-189, 2002.

3. Cesare S., *Performance requirements and budgets for the gradiometric mission.* Technical Note, GO-TN-AI-0027, Alenia Spazio, Turin, Italy, 2002.

4. ESA, *Gravity Field and Steady-State Ocean Circulation Mission*, ESA SP-1233 (1), ESA Publication Division, c/o ESTEC, Noordwijk, 1999.

5. Jekeli C., *The determination of gravitational potential differences from satellite-to-satellite tracking*, Celestial Mechanics and Dynamical Astronomy, vol. 75, 85-101, 1999.

6. Migliaccio F. and Sansò F., *Data Processing for the Aristoteles Mission*, Proceedings of the Italian Workshop on the European Solid-Earth Mission Aristoteles, Trevi, 30-31 May 1989.

7. Migliaccio F. and Reguzzoni M., *Gravity from space: the state of space-wise approach*, Proceedings of the 1st Workshop on International Gravity Field Research, Graz, 8-9 May 2003, in print.

8. Migliaccio F., Reguzzoni M. and Sansò F., *Spacewise approach to satellite gravity field determination in the presence of coloured noise*, submitted to Journal of Geodesy.

9. Migliaccio F., Reguzzoni M., Sansò F. and Tscherning C.C., *Collocation versus numerical integration in GOCE data analysis*, submitted to Journal of Geodesy.

10. Migliaccio F., Reguzzoni M., Sansò F. and Zatelli P., *GOCE: dealing with large attitude variations in the conceptual structure of the space-wise approach*, in this volume.

11. Rummel R., van Gelderen M., Koop R., Schrama E., Sansò F., Brovelli M., Migliaccio F. and Sacerdote F., *Spherical harmonic analysis of satellite gradiometry*, Netherlands Geodetic Commission Publications on Geodesy, New Series, N. 39, 1993.

12. Sansò F. and Tscherning C.C., *Fast spherical collocation: theory and examples*, Journal of Geodesy, vol. 77, 101-112, 2003.

13. Tscherning C.C., *Testing frame transformation, gridding and filtering of GOCE gradiometer data by Least-Squares Collocation using simulated data*, submitted proceedings of the IUGG General Assembly, Sapporo, July 2003.

14. Visser P.N.A.M., Sneeuw N. and Gerlach C., *Energy integral method for gravity field determination from satellite orbit coordinates*, Journal of Geodesy, vol. 77, 207-216, 2003.